Acta Biochim Biophys Sin, 2015, 47(10), 815–823
doi: 10.1093/abbs/gmv060
Advance Access Publication Date: 18 July 2015
Original Article

Original Article

Viral suppression function of intracellular antibody against C-terminal domain of rabies virus phosphoprotein

Yang Liu†, Lina Sun†, Pengcheng Yu, Aqian Li, Chuan Li, Qing Tang, Dexin Li, and Mifang Liang*

Key Laboratory for Medical Virology, NHFPC, National Institute for Viral Disease Control and Prevention, China CDC, Beijing 102206, China

†These authors contributed equally to this work.
*Correspondence address: Tel: +86-10-58900822; Fax: +86-10-58900823; E-mail: mifangl@vip.sina.com

Received 12 May 2015; Accepted 10 June 2015

Abstract

Rabies virus (RV) causes a fatal disease in both human and animals. The disease can be prevented by post-exposure prophylaxis in individuals exposed to RV. However, the neutralization effect is limited after the virus enters into the host cells. So, it is important to identify new targets for rabies therapy. In this study, a human antibody RV1A2 specific to RV phosphoprotein (RV-P) was generated from a human naïve immune antibody library. The antibody recognized all forms of the phosphoproteins including the full length (P1) and short length of the P proteins (P2, P3, P4, and P5). The epitope mapping and the molecular docking of antigen–antibody complex showed that the antibody targets at a conserved epitope of 'VLGWV' ranging from amino acid (aa) 262 to 266 at C-terminal domain of the P protein, which locates at a hydrophobic pocket region in the C-terminal of the RV-P. The aa W265 within the epitope is on the flat surface of the domain, suggesting that it may be a critical amino acid for the functions of the P protein. Our results further showed that intracellular antibody RV1A2 which targets at the C-terminal domain of the P protein could effectively inhibit RV propagation 2–4 days post infection. These results suggest that the conserved C-terminal domain may be used as a new target for drug discovery, which highlights an intracellular inhibition of RV propagation and provides a potential novel way to treat RV infection.

Key words: rabies virus (RV), rabies virus phosphoprotein (RV-P), intracellular antibody (intrabody), human fab library, single-chain variable fragment (scFv)

Introduction

Rabies is a zoonotic viral disease which usually occurs in wild as well as domestic animals [1]. It is caused by rabies virus (RV), which can infect both human and animals. As a highly neurotrophic virus, RV initially replicates in the peripheral striated skeletal muscle cells and then enters the nerve terminals or directly infects the connected motor neurons with the potential receptor nicotinic acetylcholine receptor (nAchR) [2]. However, rabies can be prevented by immediate post-exposure prophylaxis (PEP) through the combined administration of a rabies vaccine and rabies immune globulin according to the guidelines recommended by the World Health Organization (WHO). If PEP is applied correctly, it is essentially 100% effective in preventing the disease. If the WHO guidelines are not strictly followed or no PEP is applied, victims will eventually get infected with typical clinical signs of rabies. At this stage, recovery is extremely rare and the application of passive immunity is contraindicated. Therefore, novel approaches which are safe and effective for rabies PEP and therapy are urgently needed. Intracellularly expressed antibodies (intrabodies) with small molecular size and high stability are more specific toward target proteins than gene silencing

and RNA interference strategies, although the development of intrabodies is more time-consuming. The most common design of intrabody is a single-chain variable fragment (scFv) which contains a heavy-chain variable region and a light-chain variable region connected with a short linker [3]. In fact, several promising applications of scFv antibodies have already been developed [4,5].

RV belongs to the *Lyssavirus* genus of the *Rhabdoviridae* family. Its genome consists of a single negative-stranded RNA molecule encoding five viral structural proteins in the order of 3′-N-P-M-G-L-5′ [6,7]. As a modularly organized protein, RV phosphoprotein (RV-P) contains structured and disordered regions [8,9] and shows prominent structural flexibility after post-translational modification. The full-length RV-P (P1) and four amino-terminally truncated forms of RV-P (P2, aa 20-297; P3, aa 53-297; P4, aa 69-297 and P5, aa 83-297) are translated by a leaky ribosomal scanning mechanism [10]. All these RV-Ps can be found in infected cells, purified virus, and cells transfected with a plasmid encoding the complete RV-P [11]. RV-P has multiple functions in the RV-infected cells due to the presence of multiple forms of RV-Ps. RV-P is involved in encapsidating viral genome RNA, in assisting RNA-dependent RNA polymerase in the process of transcription and translation [12] and in inhibiting intercellular antiviral system mediated by interferons [13].

As RV-P is crucial for viral replication, specific antibodies against RV-P may be good candidates to inhibit RV replication. In the present study, a human antibody RV1A2 specific to the C-terminal domain of RV-P was generated from a human naïve immune antibody library, and the critical epitope of the antibody was defined. The intracellular antibody was expressed in mouse neuroblastoma (MNA) cells and the RV viral suppression function of this intrabody was tested and evaluated. Our results demonstrate an intracellular inhibition of RV propagation by this intrabody in MNA cells, which may provide a potential novel approach for the treatment of RV infection.

Materials and Methods

Virus, cells, bacterial strains, vectors, enzymes, and antibodies

RV strain CVS-11 was obtained from the National Institute of Infectious Diseases (NIID, Tokyo, Japan). MNA cells and HEK 293T cells were from American Type Culture Collection (ATCC, Manassas, USA). Bacterial strains *Escherichia coli Xli-Blue* and helper phage *VCSM13* used for antibody library construction were purchased from Invitrogene (Carlsbad, USA). Fab antibody phagemid vector pComb 3H, IgG antibody expressing vectors and scFv expressing vectors PEF/myc/cyto were prepared in our own laboratory. Purified RV virion (strain AG) was purchased from ZhongKe Biopharm (Beijing, China). Positive serum was from a healthy donor vaccinated with RV vaccine. Mouse monoclonal anti-His antibody used for positive control was purchased from AbMax Biotechnology (Beijing, China). The enzymes *Xba*I, *Sac*I, *Xho*I, and *Spe*I were purchased from New England Biolabs (Ipswich, USA). Anti-human antibody and anti-mouse antibody were purchased from Sigma (St. Louis, USA). Human CR57-IgG antibody [14] and human IgG antibody L13F3 to hantavirus used in the study were from our laboratory [15].

Generation of human Fab antibodies to RV-P

To generate the antibody to RV-P, a human naïve phage display antibody library was constructed and screened as previously described [16–18]. Briefly, lymphocytes were isolated by centrifugation from blood samples of five donors immunized with rabies vaccine. The ethical protocol was approved by the Ethics Committee of the Chinese Center for Disease Control and Prevention and written informed consent was provided by all the donors. Total mRNA was extracted from ~1×10^7 lymphocytes using an RNeasy Mini kit (Qiagen, Hilden, Germany). The cDNA was synthesized by Transcriptor High Fidelity cDNA Synthesis kit (Roche Diagnostics GmbH, Mannheim, Germany). The antibody genes of light and heavy chains were amplified with the primer pairs from 5 VK, 8 VL, and 8 VH gene family as previously described [17].

Both the light- and heavy-chain genes were cloned into the phagemid vector pComb3H [19] and multiple transformations were performed. Finally, the library size was calculated and the diversity of the library was evaluated and confirmed by sequencing of over 500 randomly selected clones. Then, the library was packaged and used for the subsequent screening. The screening procedure was performed by coating of Maxisorp Immunitube (Nunc, Roskilde, Denmark) with purified CTN virions at 4°C overnight [17]. Then, the tube was incubated with the phage library at 37°C for 2 h and washed 10 times with PBS-T solution (pH 7.4, 0.02 M, 0.05% Tween-20). Two more rounds of panning were carried out to select high-affinity Fab antibody phages using lower concentrations of coating CTN virions with more times of washing. Residual phages in the tube that were bound to virions were washed off with glycine–HCl (pH 2.2) and used to infect log-phase *E. coli* Xli-Blue plated on 2 × YT-A$^+$ agar plates. Individual colonies were incubated and induced to express crude Fab antibody. The bacterial supernatant containing Fab antibody was tested by indirect enzyme-linked immunosorbent assay (ELISA) using 96-well plates coated with 0.5 mg of purified CTN virions. Horseradish peroxidase (HRP)-conjugated anti-human Fab (Sigma) was used as the secondary antibody. The Fab antibody genes of positive clones were isolated, sequenced, and aligned to V-BASE database (http://www.vbase2.org/). The selected Fab antibody genes were expressed in *E. coli* and the binding specificities were confirmed by immunofluorescence assay (IFA) and ELISA.

Generation and purification of human IgG antibody

The selected Fab clones were further converted to IgG antibody and expressed in HEK293 cells as previously reported [20]. The selected human recombinant IgG antibody to RV-P was named RV1A2-IgG. The plasmid DNA containing RV1A2-IgG antibody genes was transfected into HEK293T cells with FuGENE HD transfection reagent (Roche, Basel, Switzerland) according to the manufacturer's protocol. Two days after the transient transfection, the supernatants were harvested and the antibodies were purified by immobilized protein-A affinity chromatography according to the standard operation procedure provided by the manufacture (GE, Milwaukee, USA) for further functional analysis [17].

Expression of full-length P, N-terminal, and C-terminal truncated RV-P

The viral RNA was extracted from CTN strain with an RNeasy Mini kit (Qiagen), and was used as a template to synthesize cDNA with random hexamer primers. The N-terminal truncation mutations of RV-P were generated by deletions including the in-frame ATG at the 5′ end of the RV-P gene [P2(ΔN19), P3(ΔN52), P4(ΔN68), VR-RV P5 (ΔN82)]. Five C-terminal RV-Ps were truncated from C-terminal at every 20 amino acids (PΔC20, PΔC40, PΔC60, PΔC80, PΔC100), and then another four C-terminal truncation mutations named as PΔC23, PΔC27, PΔC31, PΔC36 were generated. All mutations were generated using vector VR1012 with a His-tag as the template. The

full-length phosphoprotein (P1) and all recombinant phosphoprotein expression vector plasmids were transfected into HEK293T cells with FuGENE HD transfection reagent (Roche) according to the manufacturer's protocol. The cells were further analyzed by IFA and western blot analysis 48 h after transfection.

Indirect IFA

IFA was used to detect RV-infected cells, including MNA cells, BHK-21 cells, BSR cells, HEK293T cell expressing RV-P, MNA cells expressing RV-P, and Sf9 cells expressing RV-G. The cells (MNA, HEK293T, and BHK21 cells) were grown in T25 flask, 24- or 96-well plates (Greiner, Frikenhausen Germany) in DMEM with 10% fetal bovine serum (Invitrogen) for RV strains infection at 0.1 moi; or transfection with full-length or truncated RV-P plasmids DNA. Cells were either directly stained in the wells or prepared as monolayer on glass slides followed by acetone fixation. Cells were incubated with human RV1A2-IgG antibody or human CR57-IgG antibody [14] at 37°C for 30 min. Mouse anti-His monoclonal antibody was used as a positive control and an unrelated human IgG antibody L13F3 to hantavirus N protein was used as a negative control [15]. The bound antibodies were detected by fluorescein isothiocyanate (FITC)-conjugated goat anti-mouse or anti-human IgG secondary antibody with PBS dilution buffer (pH 7.4) containing 0.01% (w/v) Evans blue counterstain (Sigma). Then the stained cells were visualized under an immunofluorescence microscope (GPJ9-TS100-F; Nikon, Tokyo, Japan). Images were captured and analyzed by the software NIS-elements F 4.00.00 (Nikon, Tokyo, Japan).

Western blot analysis

The CTN virions or recombinant RV-Ps expressed HEK293T cells were lysed by lysis buffer (20 mM Tris–HCl, 500 mM NaCl, 2% Triton-X 100, pH 8.0). The total viral protein concentrations of purified CTN virions were determined by Pierce BCA Protein Assay Kit (Pierce, Rockford, USA). The lysate of purified CTN virions (lysate of 5 μg total viral proteins per lane) and recombinant RV-Ps expressed HEK293T cells (lysate of 10^4 cells per lane) were analyzed by SDS–PAGE using 4–20% and 12% Mini-PROTEAN® TGX™ Precast Gel (Bio-Rad, Hercules, USA), respectively, and then transferred to polyvinylidene fluoride (PVDF) membrane. After incubation with blocking solution (2.5% dry milk and 0.05% Tween 20 in phosphate-buffered saline) at room temperature for 1 h, the membranes were incubated overnight with RV1A2-IgG antibody at 1:1000 dilution, serum from healthy donor vaccinated with RV vaccine at 1:100 dilution or mouse anti-His monoclonal antibodies (AbMax Biotechnology) at 1:1000 dilution. After extensive washing, membranes were incubated with alkaline phosphatase conjugated-goat anti-human or anti-mouse IgG secondary antibodies (1:2000). The protein bands were finally visualized with BCIP/NBT reagent (Invitrogen) and further scanned and analyzed by Molecular Imager® Doc™ XR+ with Image Lab™ Software (Bio-Rad, Hercules, USA).

Epitope mapping by terminal truncated mutagenesis

All of the N-terminal and C-terminal truncations of RV-P with His-tag were transiently transfected into HEK293T cells. These recombinant RV-Ps were analyzed by western blot analysis with mouse anti-His monoclonal antibodies to confirm the expression of RV-Ps, and further were analyzed by western blot analysis with human RV1A2 IgG to determine the antibody-binding region.

Molecular modeling and docking of RV1A2 antibody to the C-terminal domain of RV-P

Three-dimensional data for the molecule of RV-P were obtained from the Protein Data Bank at the Research Collaboratory for Structural Bioinformatics (RCSB) (http://www.rcsb.org/) using Discovery Studio 2.0 (Accelrys, USA). Computational template-based modeling of RV1A2 was used to predict its sequence of the structure of a known antibody. A suitable template of RV1A2 was acquired by BLAST or PSI-BLAST, and alignment was sequentially and structurally performed. Then, the selected template was optimized by removing the unit cell, splitting and removing the unnecessary components such as water, ligands and ions. Homology modeling was built by running MODELER, and was analyzed and verified with Prodiles-3D and Ramachandran plots to assess and validate the quality of the model. ZDOCK was applied to dock the receptor and ligand after specifying the binding sites. RDOCK was used for the optimization of docking and the best position was selected according to the score of RMSD [16].

Generation of intracellular antibody of RV1A2 in MNA cells

The VH and VK genes of both tested antibody and negative control antibody (Antibody specific to Hantavirus N protein) were amplified and converted into scFv format fused with a short linker containing the sequence $(SGGG)_4$ by overlap extension polymerase chain reaction (PCR). Then, the ScFv genes with a 6 × His-tag were cloned into an intracellular cytoplasm expression vector PEF/myc/cyto with enzymes *Not*I and *Sal*I (Invitrogene) to generate the recombinant vector PEF/cyto/RV1A2 and control vector pEF/cyto/HTNL13F3. The vector DNAs were transfected into MNA cells in 24-well plates using FuGENE HD transfection reagent (Roche) according to manufacturer's protocol. Briefly, the MNA cells were cultured in 96-well plate at 37°C and 5% CO_2 to achieve suitable confluence. The vector DNAs of intrabody RV1A2 or intrabody L13F3 were transfected into cells with the optimum transfection ratio of plasmid amount and cell numbers (2 μg/10^5 cells). IFA was used to confirm the expression of the intrabodies with mouse anti-His antibody (AbMax Biotechnology).

Infection of intracellular antibody expressing MNA cells with RV virus

The MNA cells transfected with the above testing or control intracellular antibody genes were grown in 24-well plate. At 24 h after transfection, the cells were infected with RV strain CVS-11 at an moi of 0.1. The supernatants from each well were harvested from day 1 to day 4 post infection at 24 h interval for the subsequent viral suppression analysis. Finally, cells were fixed and stained with FITC-conjugated anti-rabies nucleoprotein antibody (anti-RVN; FujiRebio Diagnostic Company, Tokyo, Japan) to check the virus infection. To check the intracellular antibody expression, the cells were stained with mouse anti-His antibody (AbMax Biotechnology) followed by the detection with FITC-conjugated goat anti-mouse IgG (Sigma). Cells were visualized and images were captured with an immunofluorescence microscope.

Identification of viral suppression function of intercellular antibody

MNA cells were seeded in a 96-well plate at a density of 4–4.5 × 10^4 cells in each well and incubated at 37°C with 5% CO_2 for 24 h. Then the supernatants collected above were serially diluted (1:10) and inoculated into the individual wells. Each dilution of the supernatant was performed in four replications. At 48 h after the inoculation,

Table 1. Amino acid sequence of the complementary determining region of RV1A2

Antibody	VR[a]	CDR1[b]	CDR2	CDR3
RV1A2	VH1	GYIFDSYA	INGANGNR	ARGHPLAWPLDF
	VK4	QSVLSASNNKNY	GAS	QHYFSNPAT
RV1G4	VH1	GYIFDSYA	INGANGNR	ARGHPLAWPLDF
	VK1	QTISSW	KAS	QQYNSYPLT

[a]Variable region; VH, heavy chain in VR; VK, light chain in VR.
[b]Complementarity determining region.

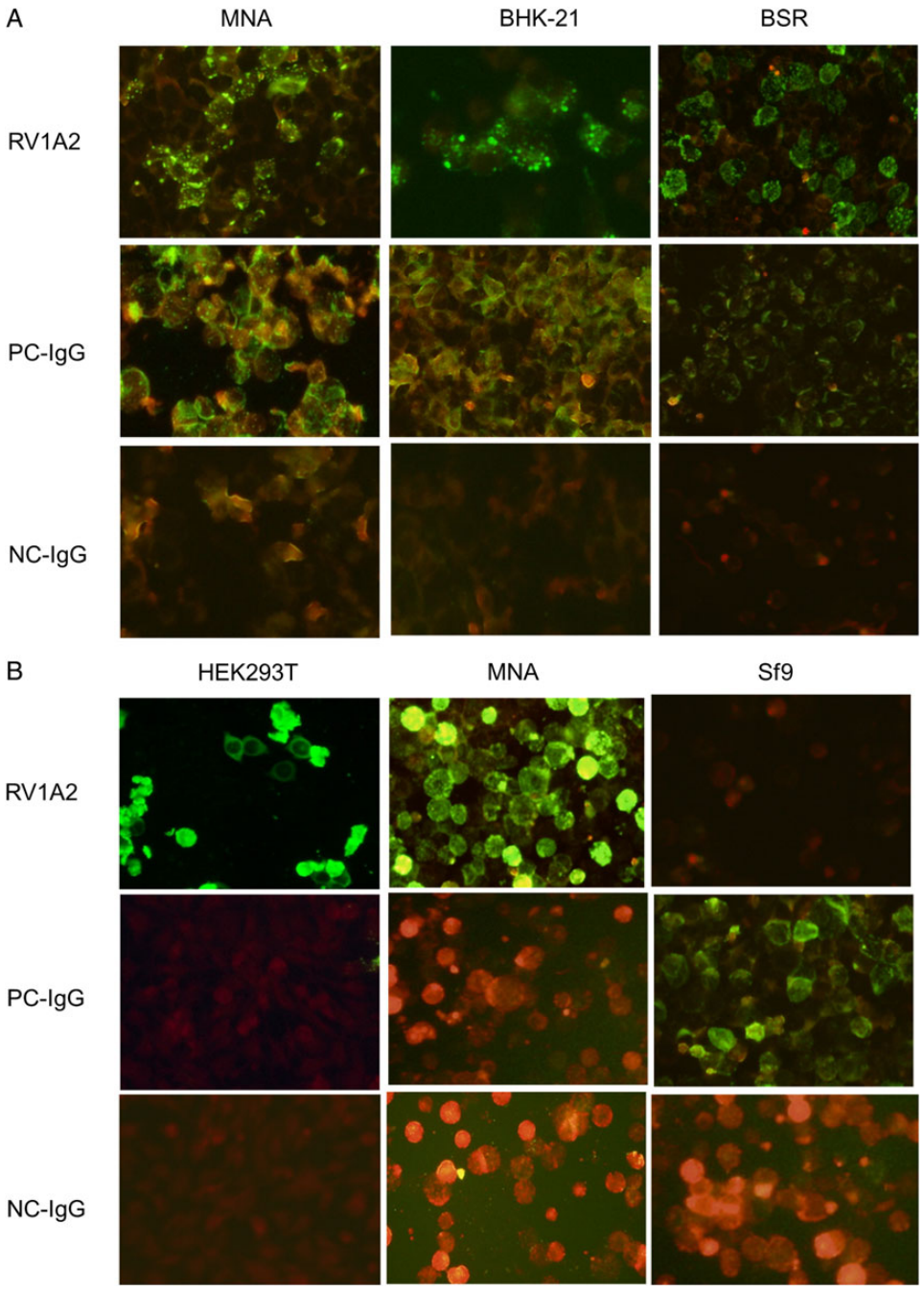

Figure 1. Binding specificity of RV1A2 IgG antibody by indirect IFA (A) Specific immunofluorescence of RV1A2 IgG antibody in RV infected MNA, BHK-21, and BSR cells (Up); CR57 antibody (PC-IgG) to RV-G was used as positive control (middle) and L13F3 antibody to hantavirus (NC-IgG) was used as negative control (bottom). (B) RV-P specific immunofluorescence of RV1A2 in RV-G expressed HEK293T and MNA cells and negative staining in RV-G expressed Sf9 cells (Up); CR57 IgG antibody (PC-IgG) as positive control to RV-G and negative control to RV-P (middle); L13F3 antibody (NC-IgG) as negative control to all tested cells. All above-bound antibodies were detected by using FITC-conjugated goat anti-human IgG antibody with PBS dilution buffer containing 0.01% (*w/v*) Evans blue counterstain.

the cells were fixed and stained with FITC-conjugated anti-RVN antibody (FujiRebio Diagnostic, Japan) to calculate focus forming unit (FFU) of each supernatant [3]. The final titer of the supernatant was determined according to the Reed & Muench formula [21]. The inhibitory effect was then calculated from the ratio of the virus titer with pre-expression of intrabody RV1A2 to that of negative control intrabody L13F3: $(1–10^{\text{RV1A2 titer}}/10^{\text{L13F3 titer}}) \times 100\%$.

Results

Generation of a human recombinant antibody RV1A2 targeting at RV phosphoprotein

A combinatorial Fab antibody library, prepared from 5 RV vaccinated heath donors, was constructed and screened with purified RV virions. The library contains four independent electro-transformations with a complexity of over 1×10^7 clones, ≥90% segment inserting and ≥90% genes diversity after sequence confirmation. After three rounds of phage panning against RV, 19 of the 500 clones were positive in binding to RV, but negative in binding to RV glycoprotein. Sequence analysis of all these positive Fab clones revealed 2 unique sequences, represented by clone 1A2 and clone 1G4, both sharing the same VH and similar VL chain genes by aligning the sequences to VBASE2 database. They were classified into VH1 and VK1 family, respectively. The deduced amino acid sequences of the two antibody CDR regions were shown in Table 1. But the binding affinity of Fab antibody 1A2 was 200 times higher than that of the Fab antibody 1G4 (data not shown). Then, the Fab-RV1A2 was selected and converted into IgG molecule for further characterization. Results demonstrated that the human IgG antibody RV1A2 recognized RV-infected BHK-21, BSR and MNA cells, as well as the RV RV-P gene-transfected MNA cells and HEK 293T cells as shown by the specific fluorescence (**Fig 1**), but could not recognize Sf9 cells expressing RV glycoproteins (**Fig. 1B**).

To confirm the specificity of the newly gained antibody RV1A2, SDS–PAGE and western blot analysis were performed using purified virions. Results showed that the antibody RV1A2 recognized only the phosphoprotein bands locating at about 30–45 kDa, while the human polyclonal antibodies (RV vaccinated health donor serum) interacted with all virus structural proteins, including glycoprotein, nucleoprotein phosphoprotein, and matrix protein (**Fig. 2A**). Furthermore, HEK293T cells were transfected with RV-P genes and tested with both RV1A2 and mouse anti-His antibody. As shown in **Fig. 2B**, antibody RV1A2 had a wide binding spectrum against PV-P, interacting not only with the full-length RV-P (P1) but also with the truncated phosphoproteins (P2, P3, and P4). Several positive protein bands were found around 30–45 kDa, indicating that the translation of N-terminally RV-P truncations were initiated from downstream AUG codons by a leaky scanning mechanism. The intensity of the P proteins bands were relatively low when stained with anti-His antibody compared with the bands stained directly with RV1A2, but it still showed the positive results.

Epitope mapping and molecular docking

Both the N- and C-terminal domains of RV-P were chosen for epitope mapping. Full-length RV-P (P1) and both N-terminal truncations (P2, P3, P4, and P5) and C-terminal truncations (PΔC20, PΔC40, PΔC60, PΔC80, PΔC100) of RV-P with His-tag were transiently transfected into HEK293T cells and analyzed by western blot analysis. As shown in **Fig. 3**, the human antibody RV1A2 recognized the full-length RV-P (P1), as well as the naturally shortened P2, P3, P4, and P5 that were expressed from the ATGs at the positions of 19, 52, 62, and 68 nucleic acid of the N-terminal. With truncations from C-terminal, it was found that RV1A2 only reacted with PΔC20, but not with other truncations: PΔC40, PΔC60, PΔC80, or PΔC100, suggesting that the linear epitope of RV1A2 was limited to the region from ΔC20 to ΔC40. Furthermore, when the deletions of every four amino acid were narrowed from ΔC20 to ΔC40 of C-terminal, it was found that RV1A2 only recognized the truncation of PΔC36 (**Fig. 3**), indicating that the linear epitope site is from 262 to 266 (VLGWV) of the C-terminal.

In order to know how the antibody interacts with the RV-P, in particular the C-terminal, molecular docking of the antibody–antigen

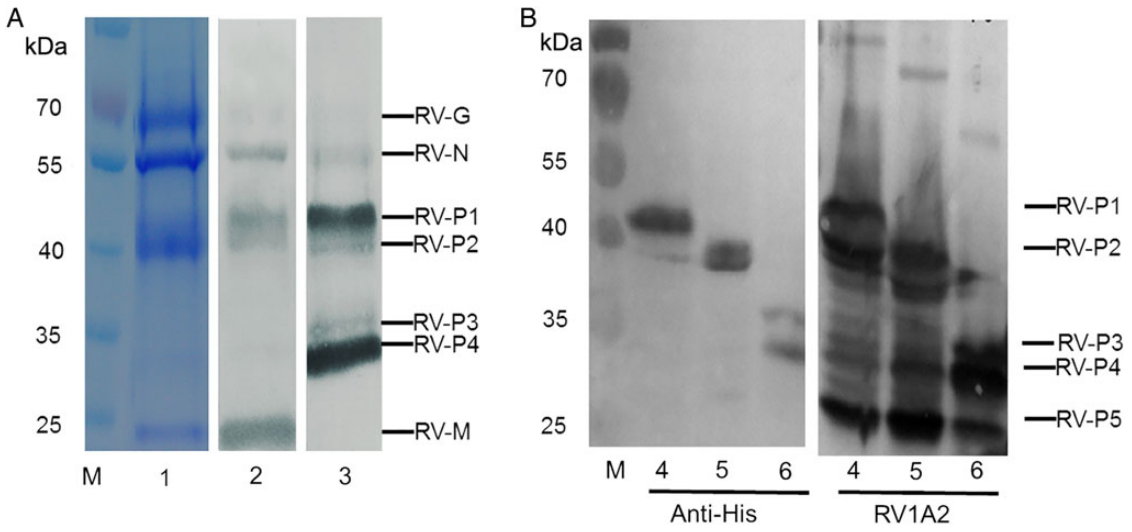

Figure 2. Identification of RV1A2 binding to RV-P by western blot analysis (A) Identification of purified virions by SDS–PAGE (lane 1) and by western blot analysis using serum from healthy donor vaccinated with RV vaccine (lane 2) and RV1A2 (lane 3) as detection antibody. (B) Western blot analysis of recombinant full-length RV-P (lane 4), P2 (lane 5), and P3 (lane 6) using anti-His antibody to confirm the RV-P expression and using antibody RV1A2 to identify its specific binding to RV-Ps. Anti-His antibody only recognized RV-Ps with targeted length, while the detection with RV1A2 showed several more RV-Ps bands locating at about 30–45 kDa, indicating that RV1A2 could recognize full-length and other short forms of RV-Ps.

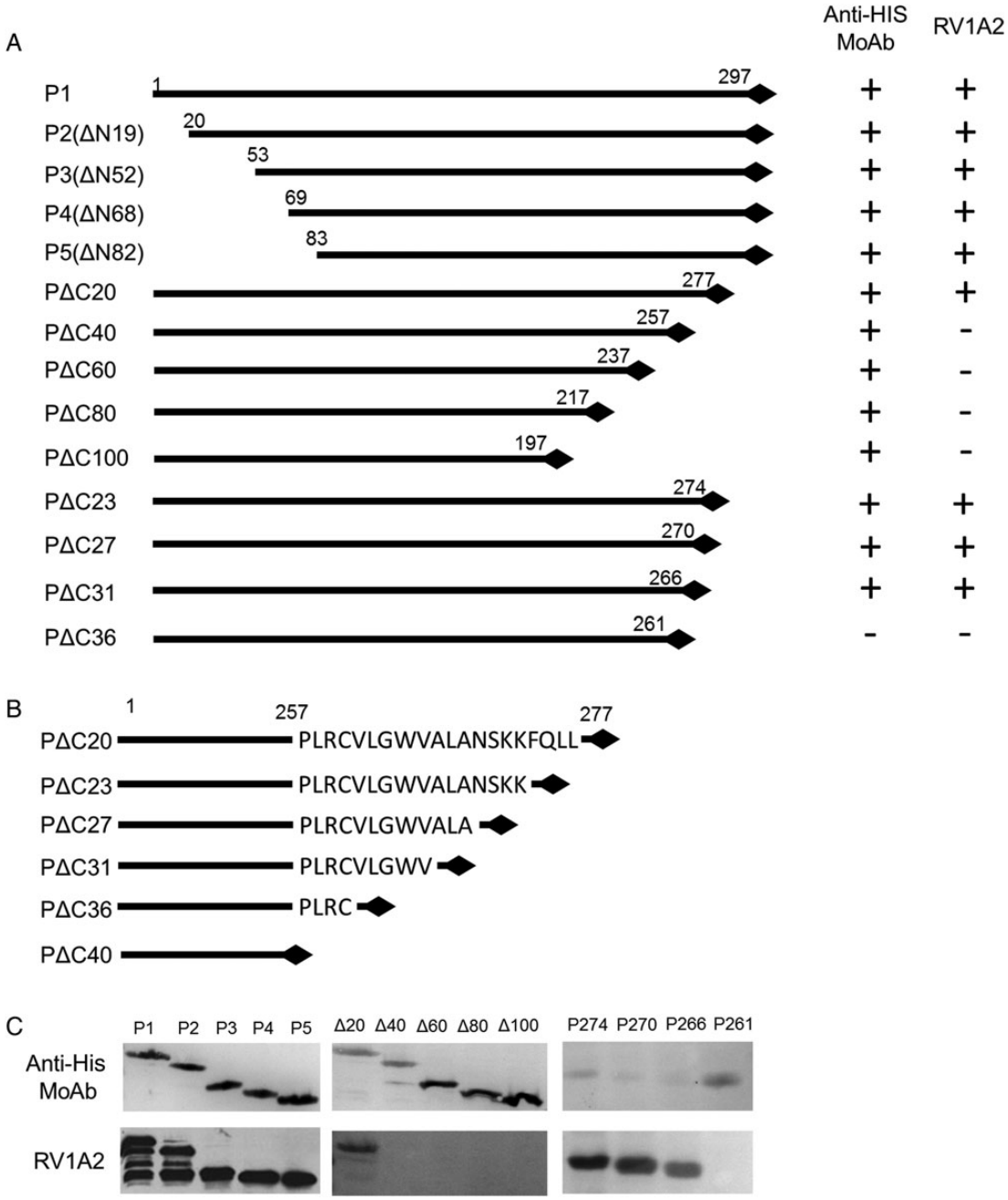

Figure 3. Epitope mapping of RV1A2 binding to RV-P (A) Schematic representation of the full-length and truncated phosphoproteins and their reactivity with anti-His-tag and RV1A2-IgG antibodies. Black bars represent the protein product of each truncated phosphoprotein with amino acid position, and filled diamonds indicate His-tag fused with proteins. (B) More details of amino acid sequences of truncated RV-Ps (PΔC20, PΔC23, PΔC27, PΔC31, PΔC36, and PΔC40). (C) Western blot analysis; top: confirmation of RV-P expression with mouse anti-His tag MAb, bottom: interaction of expressed RV-P with RV1A2-IgG antibody.

complex was analyzed using Discovery Studio 2.0. In the protein data bank (PDB), we found the crystal structures of two antibodies, 4OAW and 4JPI, which had 93.5 and 68% sequence similarity with the light chain and heavy chain of RV1A2, respectively. By using them as the model in computer simulation as shown in **Fig. 4A**, the crystal structure of 1VYI of RV-P was found in PDB. It was shown that the 'half-pear' shaped domain was the C-terminal domain (aa 186–-296) of phosphoprotein, and the computer-simulated RV1A2 just bound to the flat surface of 1VYI of RV-P. The flat face of the 'half-pear' includes a prominent hydrophobic pocket named as 'W-hole' [22], which contains many residues such as L244, P245, C261, W265, and M287. As shown in **Fig. 4B**, the critical amino acids for epitope of RV1A2 are V262, L263, G264, W265, and V266, which are indicated in the structure of 1VYI. From this docking model, the linear epitope of 'VLGWV' ranging from aa 262 to 266 of RV-P C-terminal was confirmed. In the three-dimensional structure of the epitope, only W265 (in yellow in **Fig. 4B**) was on the surface of flat face of the 'half-pear', suggesting that the position W265 may be a critical amino acid for the 'W-hole'.

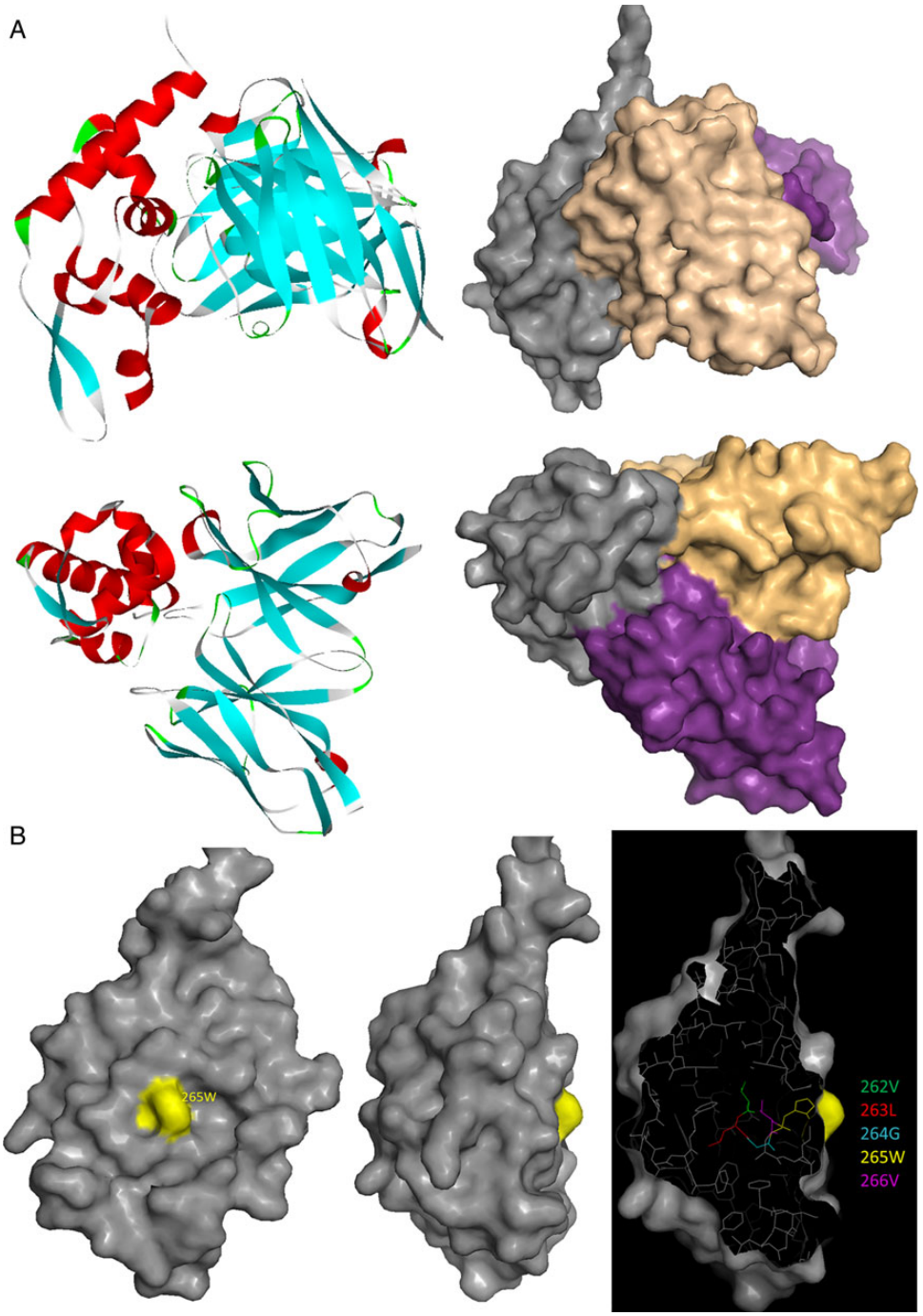

Figure 4. Molecular homology modeling and docking of RV1A2 binding to RV phosphoprotein (A) Two different viewing angles of a computer-simulated docking structure of the C-terminal domain (186–297) of RV-P; top: side view, bottom: below view, left: flat ribbon pattern, right: mesh pattern, grey: C-terminal domain of RV-P (aa 186-296), magenta: heavy chain variable region, yellow: light chain variable region. (B) View of the flat face (middle) of the C-terminal domain of RV-P as a 'half-pear' shape by 3D structure prediction (W265-hole, yellow). Critical amino acids for antibody binding, such as V262, L263, G264, W265, V266, are indicated in the modeling structure.

Viral suppression activity of intracellular antibody RV1A2

Unlike the antibodies to RV glycoprotein, the RV1A2 which targets to RV-P is not a neutralizing antibody. To evaluate the function of the antibody as well as the defined epitope, the single-chain antibody (scFv) of both RV1A2 and negative control antibody L13F3 with His-tag was efficiently expressed in MNA cells (**Fig. 5A**). Then, cells were infected with 0.05 moi of RV to check the virus suppression function. Results showed that the virus propagation was significantly inhibited after 2–4 days post infection in the presence of intracellular antibody (intrabody) RV1A2 in MNA cells, while the control intrabody L13F3 (to hantavirus N protein) did not inhibit the virus propagation (**Fig. 5**). Furthermore, results also showed that the RV virus titers from the supernatants of intrabody RV1A2 expressing MNA cells were significantly lower than that from the supernatants of MNA cells

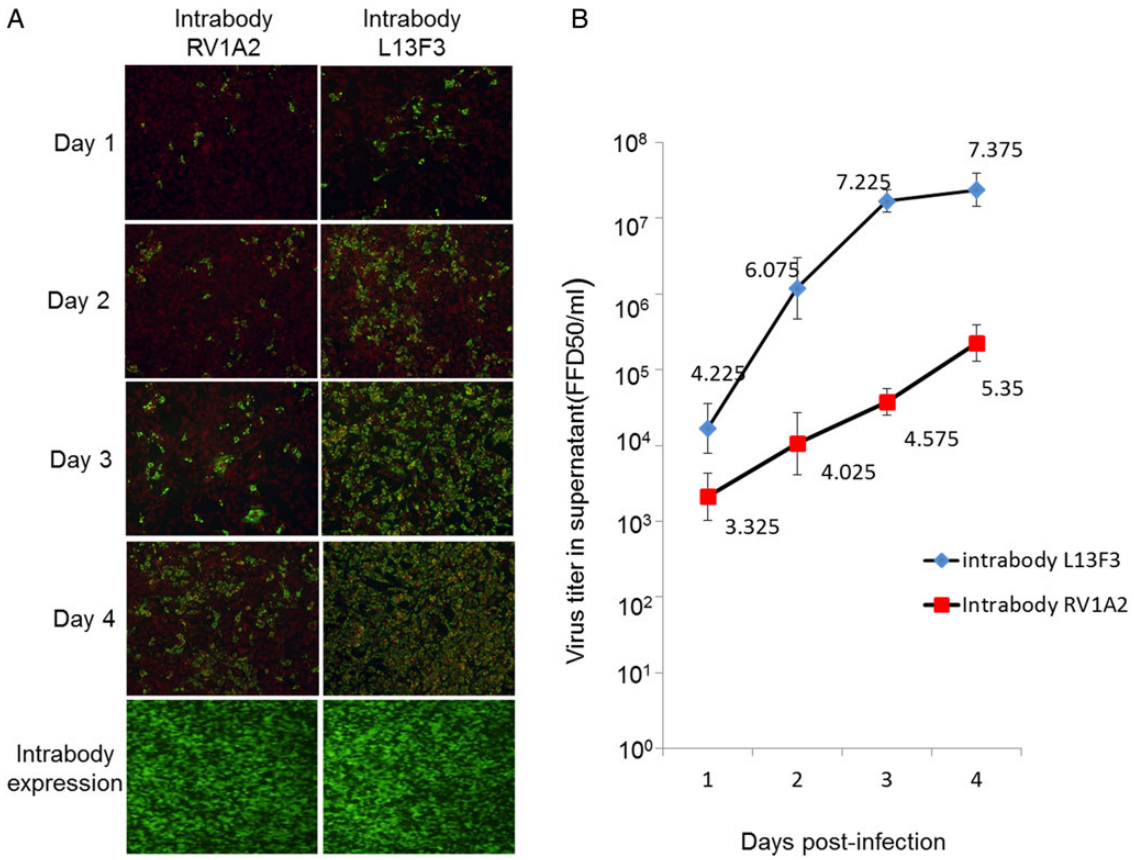

Figure 5. Inhibition function of intrabody RV1A2 and L13F3 (NC) (A) Detection of RV in MNA cells pre-expressing RV1A2 or L13F3 by indirect IFA on 1–4 d post infection. The expression levels of intrabody were shown at the bottom. (B) Reduction of virus titer by intrabody RV1A2. Time course of virus titer (FFU/ml) in supernatant of RV-infected MNA cells with expression of intrabody RV1A2 (red squares), or intrabody L13F3 (blue diamonds) was shown. Data were presented as the mean ± SD ($n = 4$). The number indicates the logarithm of the mean.

expressing the control antibody. The virus propagation was inhibited 1–4 days post infection, and the inhibition efficiency was calculated to be 90.9%, 98.4%, 98.9% and 95.9%, respectively, when compared with the control antibody (**Fig. 5B**). In summary, a viral suppression phenomenon was observed by expressing the intracellular antibody ScFv-RV1A2 in MNA cells.

Discussion

In this study, a human-derived antibody RV1A2 with a wide binding spectrum against RV-Ps was first reported. The antibody could interact with the full-length and four truncated RV-Ps through recognition of a linear epitope of 'VLGWV' ranging from aa 262 to 266 of RV-P C-terminal. Through a successful antibody–antigen docking model, we found that the epitope showed a three-dimensional structure, and only W265 located on the surface the 'half-pear' of RV-P. We presume that W265 may be a critical amino acid in the protein. Intracellular expression of the antibody showed a viral suppression activity in MNA cells.

From the previous studies, RV-P has been identified as a multifunctional regulatory protein that involves in virus transcription and replication. The presence of multiple forms of RV-Ps is due to the leaky ribosomal scanning mechanism by using differential IRES translation initiation [10]. The P1 and P2 locate in the cytoplasm, whereas P3, P4, and P5 locate in the nucleus [22]. RV-Ps have multiple functions. Recent studies have suggested that the N-terminal of RV-P plays an important role in binding to the virus polymerase L protein which is important for RNP formation [22]. An antiviral activity was observed when peptides mimicking the N-terminus of RV-P were intracellularly expressed [23]. However, the functional intracellular antibody RV1A2 originally derived from our human antibody library was defined to recognize the linear epitope of 'VLGWV' (aa 262–266) which locates at the RV-P C-terminus. The detailed three-dimensional structure of P has been obtained for its C-terminal domain [22]. The C-terminal epitope region seemed to be essential for the P protein to interact with the nucleocapsid protein (N) [24]. By limited protease digestion, a monomeric C-terminal domain of P (aa 185–297) was identified to bind to N protein in the RNP complex [22]. Binding of RV N protein through the C-terminal half of the P protein was much stronger than the interaction with N-terminal half [23]. The RV1A2 was the first human-derived RV-P antibody targeting at the C-terminal domain of the P protein. From a previous publication for RV gene evolution analysis [25], it was found that the epitope of 'VLGWV' (aa 262–266) recognized by the antibody RV1A2 is well conserved, compared with the sequences from 120 RV strains in GenBank, which are all conserved in RV type I and mostly conserved in the strains of RV type II to VII (96.2%–99.9%).

Intracellular gene- or protein-targeting therapy has different mechanisms other than neutralization. The antibody RV1A2 used in this study is not a neutralizing antibody because it targets at P protein, but the inhibition of RV replication through intracellular function might be achieved by blocking the key target, the conserved linear

epitope comprised of RV-P C-terminal residues 262–266 (VLGWV). The 'half-pear' shaped domain locates between aa 186 and aa 296 at the C-terminus of RV-P. The flat face of the 'half-pear' includes a prominent hydrophobic pocket (named as W-hole) formed by many residues such as L244, P245, C261, W265, and M287. It may be involved in the interaction between phosphoprotein and N-RNA complex [26]. For the antibody RV1A2, we presume that the antibody-binding epitope, in particular the position of W265, may contribute to the 'W-hole'. As previously reported, the 'W-hole' was also recognized by another MAb 402–13, of which, the epitope ranges from aa256 to 297 of C-terminal domain [24]. The C-terminal might be able to bind with the nucleoprotein (N)-RNA template important for transcription and replication steps in virus life cycle [24]. Further investigations are needed to clarify whether the multiple functions of RV-P are through its interactions with other viral proteins or with intracellular signal pathway molecules.

Our evaluation of RV1A2 on inhibiting RV propagation is preliminary. The role and mechanism of RV1A2 and/or its recombinant derivatives in the inhibition of RV propagation need to be further investigated. Currently, we are in the process of further analysis by using alternative methods such as western blotting to determine the level of translations of viral proteins and using qRT-PCR to detect the level of viral transcription and replication. A more stable and reliable expression and delivery system will be helpful in the future studies. In addition, it will be a great challenge in intrabody therapeutic research to achieve effective penetration of membrane barriers, particularly across the highly resistant blood-brain barrier, which is crucial for successful intracellular targeting.

Funding

This work was mainly supported by a grant from the National Science and Technology Major Project for Infectious Diseases (No. 2013ZX10004-101).

References

1. Rupprecht CE, Hanlon CA, Hemachudha T. Rabies re-examined. *Lancet Infect Dis* 2002, 2: 327–343.
2. Israsena N, Mahavihakanont A, Hemachudha T. Rabies virus infection and microRNAs. *Adv Virus Res* 2011, 79: 329–344.
3. Kaku Y, Noguchi A, Hotta K, Yamada A, Inoue S. Inhibition of rabies virus propagation in mouse neuroblastoma cells by an intrabody against the viral phosphoprotein. *Antiviral Res* 2011, 91: 64–71.
4. Smith AJ. New horizons in therapeutic antibody discovery: opportunities and challenges versus small-molecule therapeutics. *J Biomol Screen* 2015, 20: 437–453.
5. Mitragotri S, Burke PA, Langer R. Overcoming the challenges in administering biopharmaceuticals: formulation and delivery strategies. *Nat Rev Drug Discov* 2014, 13: 655–672.
6. Gerard FC, Ribeiro Ede A Jr, Leyrat C, Ivanov I, Blondel D, Longhi S, Ruigrok RW, *et al*. Modular organization of rabies virus phosphoprotein. *J Mol Biol* 2009, 388: 978–996.
7. Nishizono A, Yamada K. [Rhabdoviruses]. *Uirusu* 2011, 62: 183–196.
8. Le Mercier P, Jacob Y, Tanner K, Tordo N. A novel expression cassette of lyssavirus shows that the distantly related Mokola virus can rescue a defective rabies virus genome. *J Virol* 2002, 76: 2024–2027.
9. Nadin-Davis SA, Fehlner-Gardiner C, Sheen M, Wandeler AI. Characterization of a panel of anti-phosphoprotein monoclonal antibodies generated against the raccoon strain of rabies virus. *Virus Res* 2010, 152: 126–136.
10. Chenik M, Chebli K, Blondel D. Translation initiation at alternate in-frame AUG codons in the rabies virus phosphoprotein mRNA is mediated by a ribosomal leaky scanning mechanism. *J Virol* 1995, 69: 707–712.
11. Gigant B, Iseni F, Gaudin Y, Knossow M, Blondel D. Neither phosphorylation nor the amino-terminal part of rabies virus phosphoprotein is required for its oligomerization. *J Gen Virol* 2000, 81: 1757–1761.
12. Chenik M, Schnell M, Conzelmann KK, Blondel D. Mapping the interacting domains between the rabies virus polymerase and phosphoprotein. *J Virol* 1998, 72: 1925–1930.
13. Rieder M, Brzozka K, Pfaller CK, Cox JH, Stitz L, Conzelmann KK. Genetic dissection of interferon-antagonistic functions of rabies virus phosphoprotein: inhibition of interferon regulatory factor 3 activation is important for pathogenicity. *J Virol* 2011, 85: 842–852.
14. Bakker AB, Marissen WE, Kramer RA, Rice AB, Weldon WC, Niezgoda M, Hanlon CA, *et al*. Novel human monoclonal antibody combination effectively neutralizing natural rabies virus variants and individual *in vitro* escape mutants. *J Virol* 2005, 79: 9062–9068.
15. Koch J, Liang M, Queitsch I, Kraus AA, Bautz EK. Human recombinant neutralizing antibodies against hantaan virus G2 protein. *Virology* 2003, 308: 64–73.
16. Yu L, Zhang L, Sun L, Lu J, Wu W, Li C, Zhang Q, *et al*. Critical epitopes in the nucleocapsid protein of SFTS virus recognized by a panel of SFTS patients derived human monoclonal antibodies. *PLoS One* 2012, 7: e38291.
17. Sun L, Chen Z, Yu L, Wei J, Li C, Jin J, Shen X, *et al*. Generation and characterization of neutralizing human recombinant antibodies against antigenic site II of rabies virus glycoprotein. *Appl Microbiol Biotechnol* 2012, 96: 357–366.
18. Kashyap AK, Steel J, Oner AF, Dillon MA, Swale RE, Wall KM, Perry KJ, *et al*. Combinatorial antibody libraries from survivors of the Turkish H5N1 avian influenza outbreak reveal virus neutralization strategies. *Proc Natl Acad Sci USA* 2008, 105: 5986–5991.
19. Schmitz U, Versmold A, Kaufmann P, Frank HG. Phage display: a molecular tool for the generation of antibodies—a review. *Placenta* 2000, 21 (Suppl A): S106–S112.
20. Persic L, Roberts A, Wilton J, Cattaneo A, Bradbury A, Hoogenboom HR. An integrated vector system for the eukaryotic expression of antibodies or their fragments after selection from phage display libraries. *Gene* 1997, 187: 9–18.
21. Reed LJ, Muench H. A simple method of estimating fifty per cent endpoints. *Am J Epidemiol* 1938, 27: 493–497.
22. Mavrakis M, McCarthy AA, Roche S, Blondel D, Ruigrok RW. Structure and function of the C-terminal domain of the polymerase cofactor of rabies virus. *J Mol Biol* 2004, 343: 819–831.
23. Castel G, Chteoui M, Caignard G, Prehaud C, Mehouas S, Real E, Jallet C, *et al*. Peptides that mimic the amino-terminal end of the rabies virus phosphoprotein have antiviral activity. *J Virol* 2009, 83: 10808–10820.
24. Toriumi H, Honda Y, Morimoto K, Tochikura TS, Kawai A. Structural relationship between nucleocapsid-binding activity of the rabies virus phosphoprotein (P) and exposure of epitope 402–13 located at the C terminus. *J Gen Virol* 2002, 83: 3035–3043.
25. Nadin-Davis SA, Abdel-Malik M, Armstrong J, Wandeler AI. Lyssavirus P gene characterisation provides insights into the phylogeny of the genus and identifies structural similarities and diversity within the encoded phosphoprotein. *Virology* 2002, 298: 286–305.
26. Ribeiro Ede A Jr, Leyrat C, Gerard FC, Albertini AA, Falk C, Ruigrok RW, Jamin M. Binding of rabies virus polymerase cofactor to recombinant circular nucleoprotein-RNA complexes. *J Mol Biol* 2009, 394: 558–575.